# Eulerian Spectral/Finite Difference Method for Large Deformation Modelling of Visco-Elasto-Plastic Geomaterials.

Boris J.P. Kaus [a] Yuri Yu. Podladchikov [a] Daniel W. Schmid [a]

[a] *Earth Science Department, ETH Zürich, Sonnegstrasse 5, 8092 Zürich, Switzerland*

**Abstract**

Many problems that occur in geodynamics can be reduced to the solving of visco-elasto-plastic rheological equations. Here a spectral/finite-difference method is described that can deal with these rheologies in an eulerian framework. The method approximates derivatives in vertical direction by finite-differences and in horizontal direction(s) by a pseudospectral approach. Material boundaries are tracked by marker chains that are moved through a fixed grid and allow large deformations. It is demonstrated that the Gibbs effect is avoidable; the method is reliable up to large viscosity contrasts of $5 \times 10^5$ and is able to resolve strongly localised solutions like shear bands.

*Key words:* Spectral, finite difference, plasticity, viscoelasticity, interface tracking, Gibbs effect, shear banding, interface tracking

## 1 Introduction

The ultimate goal of geoscientists is to understand the physical processes that formed and reworked the earth's tectonic plates and the underlying mantle. This is a difficult problem since the current state of earth is a result of billions of years of deformation and insight in the main driving mechanisms is at least indirect or approximate.

In recent years numerical modelling has been proven useful here. Much of our understanding about mantle convection, for example, comes from numerical simulations that treat the mantle as a creeping highly viscous fluid. The lithospheric plates, on the other hand, are colder than the mantle and behave more like a viscoelastic, brittle solid. Numerical modelling of the deformation of these plates and their coupling to the mantle thus requires the solving of visco-elasto-plastic rheological equations. In addition it is important that a

*Article published in Bolletino di Geofisica (2004). Vol. 45, p346-349*

numerical method, developed for this purpose, is efficient, can handle large deformations, strong variations of material properties, free surface effects and non-linear rheologies. Previous workers utilized finite element methods (Huismans *et.al.* [1]), dynamic lagrangian remeshing methods (Braun and Sambridge [2]) and control-volume methods (Poliakov *et.al.* [3]) to deal with the problems described above.
We follow a different approach and solve the governing equations by an eulerian finite-difference/spectral method [4].

## 2 Mathematical model

For many geodynamic applications inertial effects are not important and the balance equations can be written as:

$$\begin{aligned} \frac{\partial \rho v_i}{\partial x_i} + \frac{\partial \rho}{\partial t} &= 0 \\ \frac{\partial \sigma_{ij}}{\partial x_j} &= \rho g_i \end{aligned} \tag{1}$$

here $v_i$ is velocity, $\sigma_{ij}$ stress, $\rho$ density, $g$ gravitational acceleration and $t$ is time.
A Maxwell viscoelastic rheology for stress- and strain-deviators is assumed (e.g. Schmalholz *et.al.* [4]):

$$\dot{\tilde{\varepsilon}}_{ij}^{ve} = \dot{\tilde{\varepsilon}}_{ij}^{v} + \dot{\tilde{\varepsilon}}_{ij}^{e} = \frac{1}{2\mu_{vis}}\tilde{\sigma}_{ij} + \frac{1}{2G}\frac{D\tilde{\sigma}_{ij}}{Dt} \tag{2}$$

where $\tilde{\sigma}_{ij} = \sigma_{ij} + P$, $\dot{\tilde{\varepsilon}}_{ij} = \dot{\varepsilon}_{ij} - \dot{\bar{\varepsilon}}$, $\dot{\varepsilon}_{ij} = \frac{1}{2}\left(\frac{\partial v_i}{\partial x_j} + \frac{\partial v_j}{\partial x_i}\right)$, $P = -\frac{1}{3}tr\left(\sigma_{ij}\right)$, $\dot{\bar{\varepsilon}} = \frac{1}{3}tr\left(\dot{\varepsilon}_{ij}\right)$, $G$ is the elastic shear modulus, $\mu_{vis}$ the shear viscosity (which might have a nonlinear stress- and temperature-dependence) and $\frac{D}{Dt}$ denotes the objective derivative of the stress tensor.
Rocks cannot sustain high stresses; they will fail plastically instead. Since in this case elastic strains are small it is adequate to make the additive strain rate decomposition, which states that:

$$\dot{\varepsilon}_{ij} = \dot{\varepsilon}_{ij}^{ve} + \dot{\varepsilon}_{ij}^{p} \tag{3}$$

The plastic strain rate can be calculated according to:

$$\dot{\varepsilon}_{ij}^{p} = \dot{\lambda}\frac{\partial Q}{\partial \sigma_{ij}} \tag{4}$$

where $\frac{\partial Q}{\partial \sigma_{ij}}$ is the direction of plastic flow and $\dot{\lambda}$ the plastic multiplier. The yield criterion can be expressed in Kuhn-Tucker form as

$$\dot{\lambda} \geq 0, F \leq 0, \dot{\lambda} F = 0 \tag{5}$$

For rocks under upper-crustal conditions, a Mohr-Coulomb yield function with non-associated flow rule is the minimum model. Spelled out for a 2D case it can be written as:

$$\begin{aligned} F = \tau^* - \sigma^* \sin(\phi) - c\cos(\phi) \\ G = \tau^* - \sigma^* \sin(\psi) \end{aligned} \tag{6}$$

where $\phi$ is the friction angle, $\psi$ the dilation angle (in general smaller than $\phi$ ), $c$ the cohesion of the rocks, $\tau^*$ is the radius and $\sigma^*$ the centre of the Mohr-circle.
By substituting Eqs. (3) and (4) into Eq. (2) we arrive at the rheological equation for a visco-elasto-plastic material:

$$\dot{\varepsilon}_{ij} - \dot{\varepsilon}_{ij}^{p} - \bar{\dot{\varepsilon}}^{ve} = \tilde{\dot{\varepsilon}}_{ij}^{ve} = \frac{1}{2\mu_{vis}} (\sigma_{ij} + P) + \frac{1}{2G} \frac{D(\sigma_{ij} + P)}{Dt} \tag{7}$$

## 3 Numerical method

The system of equations, Eq. (1) and Eq. (7), is discretised using a finite-difference/spectral approach. Differently to conventional approach leading to a $4^{th}$-order ordinary differential equation (e.g. [4]), our formulation results in two $2^{nd}$-order equations for two unknown functions. The balance equations are always satisfied analytically by choosing $\sigma_{zz}$ and $v_z$ as the primitive unknown functions. Moreover, the formulation makes the implementation of stress boundary-conditions straightforward. Variables are approximated by a Fourier series in the horizontal direction and by a finite-difference scheme in the vertical direction. The balance equations (Eqs. (1)) can than be written for a 2D case as (see e.g. Trefethen [10]):

$$\begin{aligned} i\omega \hat{v}_x^l + \frac{\partial \hat{v}_z^l}{\partial z} &= \hat{\dot{\varepsilon}}^{p} + \hat{\dot{\varepsilon}}^{ve} \\ i\omega \hat{\sigma}_{xx}^k + \frac{\partial \hat{\sigma}_{xz}^k}{\partial z} &= 0 \\ i\omega \hat{\sigma}_{xz}^k + \frac{\partial \hat{\sigma}_{zz}^k}{\partial z} &= \hat{\rho}^k g \end{aligned} \tag{8}$$

for $k = 1..nk$ and $l = 1..nl$. Here hats denote the Fourier coefficients, $\omega = 2\pi k/L$ is the wave number, $L$ the size of the domain in the horizontal direction, $i = \sqrt{-1}$ and $nk, nl$ are the total number of harmonics in the spectral direction.
From these equations, analytical expressions for $\hat{\sigma}_{xx}$ and $\hat{\sigma}_{xz}$ as a function of $\hat{\sigma}_{zz}$ can be written:

$$\begin{aligned} \hat{\sigma}^k_{xz} &= -\frac{1}{i\omega}\left(\frac{\partial \hat{\sigma}^k_{zz}}{\partial z} - \hat{\rho}^k g\right) \\ \hat{\sigma}^k_{xx} &= -\frac{1}{i\omega}\left(\frac{\partial \hat{\sigma}^k_{xz}}{\partial z}\right) = \frac{1}{i\omega}\left(\frac{\partial}{\partial z}\left(\frac{1}{i\omega}\left(\frac{\partial \hat{\sigma}^k_{zz}}{\partial z} - \hat{\rho}^k g\right)\right)\right) \end{aligned} \tag{9}$$

The same applies for $\hat{v}_x$ and $\hat{v}_z$:

$$\begin{aligned} \left(\hat{\sigma}^k_{xx} - \hat{\sigma}^k_{zz}\right) &= 2\hat{\mu}^m_{eff}\left(\left(i\omega\hat{v}^l_x - \hat{\dot{\varepsilon}}^p_{xx}\right) - \left(\frac{\partial \hat{v}^l_z}{\partial z} - \hat{\dot{\varepsilon}}^p_{zz}\right)\right) + \\ &\qquad \hat{\eta}^m_{eff}\left(\hat{\overset{\nabla}{\sigma}}{}^{k,old}_{xx} - \hat{\overset{\nabla}{\sigma}}{}^{k,old}_{zz}\right) \\ \hat{\sigma}^k_{xz} &= \hat{\mu}^m_{eff}\left(\frac{\partial \hat{v}^l_x}{\partial z} + i\omega\hat{v}^l_z - \hat{\dot{\varepsilon}}^p_{xz}\right) + \hat{\eta}^m_{eff}\left(\hat{\overset{\nabla}{\sigma}}{}^{k,old}_{xz}\right) \end{aligned} \tag{10}$$

where $\mu_{eff} = \frac{1}{\frac{1}{\hat{\mu}_{vis}} + \frac{1}{\hat{G}dt}}$ and $\eta_{eff} = \frac{1}{1 + \frac{\hat{G}dt}{\hat{\mu}_{vis}}}$ are redefined effective viscosities (which become dependent on the timestep $dt$). $\nabla$ denotes the objective Jaumann derivative of the stress component, which consists of an advective and a rotational part:

$$\overset{\nabla}{\sigma}{}^{old}_{ij} = \left(v_i \frac{\partial \sigma^{old}_{ij}}{\partial x_i} + rotation(\sigma^{old}_{ij}\right) \tag{11}$$

Advective terms are solved using a characteristics-based method (Malevsky and Yuen [9]) in order to minimize numerical diffusion, whereas the rotational terms are modelled using standard rotational formulas (Turcotte and Schubert [5]) that collapse into the Jaumann corotational derivative in the case of small rotations. Two equations for the two unknowns $\hat{\sigma}_{zz}$ and $\hat{v}_z$ are obtained by combining eqs. (9)-(12). Solving these equations is straightforward if the viscosity is constant or depth-dependent. If there are strong lateral gradients of effective viscosity, the algorithm finds the solution iteratively (Schmalholz et. al. 2001). If there are strong lateral gradients of effective viscosity, the algorithm finds the solution iteratively (Schmalholz et. al. [4]). The method converges even for large viscosity contrasts of $5\times10^5$, without noteworthy Gibbs effect (see Figure 1a).

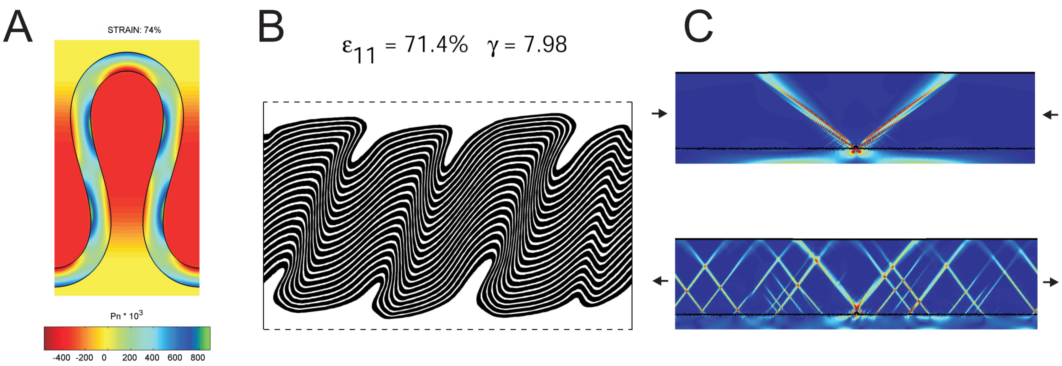


Fig. 1. Numerical examples: A) Pressure distribution in a pure-shear fold with a viscosity contrast of $5 \times 10^5$ (Schmalholz et. al. [4]). B) Multilayer sequence (viscosity contrast 1000) subjected to pure-and simple shear deformation (Schmid [11]). C) Localised deformation in a Mohr-Coulomb brittle material with a friction angle of 30 and a dilation angle of 0 degrees, subjected to pure-shear bulk deformation.

The current formulation makes it straightforward to implement no-slip or free-slip boundary-conditions. In addition, the implementation of stress-free boundary-conditions or any condition involving normal stresses does not require $3^{rd}$ derivatives. A free surface boundary condition is difficult to incorporate in eulerian fixed grid numerical codes such as the one described here. Therefore we approximate the free surface by putting a layer of low viscosity in the upper part of the numerical box.

Boundaries between materials with a sharp variation of properties are described by marker-chains that are moved through a fixed computational grid by an implicit time step algorithm (see Figure 1b for an example of simple-shear folding). Fourier coefficients of effective viscosity and density fields are calculated directly from the marker-chain. An advantage of such a marker-chain method over particle-based methods is that much less points are needed to describe a material like a fold. In the case that more slowly varying properties like temperature have to be advected, a characteristics-based method is employed (e.g. Malevski and Yuen [9]).

Plastic yielding occurs if stresses are higher than the yield envelop (i.e. $F > 0$ in equation (6)).)). If this is detected, stresses are pointwise returned to the yield envelop in the direction of the plastic flow (equation 4). Combining a Mohr-Coulomb yield envelop with a Mohr-Coulomb plastic flow potential results in shear bands with angles that are in-between the Roscoe angle $(45 - \psi/2)$ and the Coulomb-angle $(45 - \phi/2)$, which is in agreement with theoretical predictions (e.g. Vermeer [8]).

## 4 Conclusions

The Eulerian spectral/finite difference method is a promising tool for modeling geodynamic problems, since it can deal with large deformations. An algorithm such as the one described in this paper reduces a 2D or a 3D problem to the subsequent solving of 1D equations (see e.g. Schmalholz et. al. 2001 and Kaus and Podladchikov 2000), which is efficient even in the case with strongly varying material properties. Examples (Figure 1) illustrate the capability of the method to deal with large deformations, strongly varying material properties and non-associated Mohr-Coulomb plasticity.

## References


[1] Huismans, R.S., Podladchikov, Y.Y. and Cloetingh, S. The Transition from passive to active rifting, relative importance of asthenospheric doming and passive extension of the lithosphere. *JGR* (2001). **106 B6**: 11,271–11,292.

[2] Braun, J. and Sambridge, M. Dynamical Lagrangian Remeshing (DLR): A new algorithm for solving large strain deformation problems and its application to fault-propagation folding. *EPSL* (1994). **124**: 211–220.

[3] Poliakov A., Podladchikov Yu., Dawson E. and Talbot C. Salt diapirism with simultaneous brittle faulting and viscous flow. *Geological Society Special Publication* (1996). **100**: 291–302.

[4] Schmalholz, Podladchikov, Schmid. A spectral/finite-difference method for simulating large deformations of heterogeneous, viscoelastic materials. *GJI* (2001). **145**: 188–208.

[5] Turcotte and Schubert. *Geodynamics* (Cambridge University Press, 1982).

[6] Kaus, B.J.P., Podladchikov, Yu.Y. Forward and reverse modeling of the three-dimensional viscous Rayleigh-Taylor instability. *GRL* (2000); **28**(6): 1095–1098.

[7] Christensen, Harder. 3D convection with variable viscosity. *GJI* (1991); **104**: 213–226.

[8] Vermeer , Geotechnique, 40(2), 223-236.

[9] Malevsky and Yuen (1991), Physics of Fluids, A3(9), 2105-2115.

[10] Trefethen. *Spectral methods in MATLAB* (SIAM, 2001).

[11] Schmid, D. W. *Finite and infinite heterogeneities under pure and simple shear.* (unpublished PhD thesis ETHZ, 2002).